Theoretical and Applied Climatology (2021) 144:1297–1310
https://doi.org/10.1007/s00704-021-03600-5

ORIGINAL PAPER

Changes in water use efficiency and their relations to climate change and human activities in three forestry regions of China

Jiaxi Tian[1] · Zengxin Zhang[1,2] · Rui Kong[2] · Bin Zhu[1] · Fengying Zhang[1] · Shanshan Jiang[3] · Xi Chen[3]

Received: 13 July 2019 / Accepted: 17 March 2021 / Published online: 31 March 2021

Abstract
Water use efficiency (WUE) is an important link between carbon and water cycles, which is critical for the forests under future global climatic changes. WUE_{NDVI} was calculated by accumulated normalized difference vegetation index (NDVI) and actual evapotranspiration (ET) and could reflect the impacts of climatic changes and human activities on WUE. The three forestry regions of China are the northeast, southwest, and southeast areas. Among them, the northeast forest region is a natural forest region with forest stock accounting for more than 1/4 of China, and the southwest mountainous forest region is another natural forest region in China, with forest stock accounting for more than 1/3 of China, while the southeast forest area is mainly plantations. In 2018, the forest areas over three forestry regions of China were around 1,725,988 km^2. This paper evaluated the changes in forest WUE and their relationships with climatic change and human activities over three forestry regions of China during 1961–2019. The main findings of this study were summarized as follows: (1) the spatial changes of WUE were gentle in the artificial forest region but fluctuant sharply in the natural forest regions. In the southwest forest region, the WUE increased with elevation, while it showed the opposite trends in the artificial forest region. Overall, the annual mean forest WUE increased in almost all regions of the study areas during 1961-2019; (2) in the northeast and southeast forest regions, the WUE presented a negative relationship with the temperature. In the southwest forest region, the WUE was positively correlated with the temperature and its increase rate slowed down significantly when the temperature increases by more than 1 °C. The WUE was negatively correlated with precipitation in the three regions and was more sensitive to the decrease of precipitation. The sensitivity of WUE to precipitation reduction was highest in the artificial forest region and lowest in the northeast forest region; (3) the forest WUE and WUE_{NDVI} were lowest in the artificial forest region but highest in the northeast forest region, while the net increase in forests area during 1980–2018 was largest in the artificial forest region (155,975 km^2) but lowest in the northeast forest region (78,766 km^2). In general, human activities had the greatest impact on the forest WUE in the northeast forest region. Human activities and climatic change had quite complex and interactive effects on forest WUE. Therefore, more attention should be paid to the joint influences of climate change and human activities on WUE.

✉ Zengxin Zhang
zzhang@hhu.edu.cn

Jiaxi Tian
tianjiaxi@njfu.edu.cn

Rui Kong
kongrui@njfu.edu.cn

Bin Zhu
binzhu@njfu.edu.cn

Fengying Zhang
zhangfengying@njfu.edu.cn

Shanshan Jiang
shantj@tju.edu.cn

Xi Chen
xichen@hhu.edu.cn

[1] Joint Innovation Center for Modern Forestry Studies, College of Biology and the Environment, Nanjing Forestry University, Nanjing 210037, Jiangsu, China

[2] State Key Laboratory of Hydrology-Water Resources and Hydraulics Engineering, Hohai University, Nanjing 210098, Jiangsu, China

[3] Institute of Surface-Earth System Science, Tianjin University, Tianjin 300072, China

1 Introduction

The forest ecosystem is a key component of the terrestrial ecosystem, which could conserve water, preventing wind, fixing sand, and even regulate the balance of climate (Morecroft et al. 1998; Shao et al. 2017). Despite forests only cover 40% of the Earth's ice-free regions, they contain about 90% of terrestrial biomass in the Earth (Shao et al. 2017). Forests also play a significant role in the global carbon cycle and provide beneficial services to society (Pan et al. 2011). In recent years, natural forests are getting more and more degraded and fragmented all over the world (Wright 2005). Therefore, many forestry strategies have been implemented worldwide in order to increase reforestation (Hanane et al. 2018). Water use efficiency (WUE) is an important link between the carbon cycle and the water cycle in forest ecosystems, which is critical for the productivity and health of plants under future global climatic changes (Xiao et al. 2004; Xu and Hsiao 2004; Niu et al. 2011). Therefore, the WUE of the forest ecosystems has great influences on the carbon and water cycle of the earth. WUE is generally defined as the ratio of net primary productivity (NPP) to actual evapotranspiration (ET), which could reflect the carbon-water cycle. NPP is the difference between the carbon absorbed by photosynthesis and released by autotrophic respiration by green plants per unit time and per unit space (Wang et al. 2009; Lieth and Whittaker 1975). The forest ecosystem NPP is a major constituent of all the terrestrial carbon budgets (Liu et al. 2015), which accounts for 65% of terrestrial NPP (Gower et al. 1996). Due to the complexity of land surface types, ET is generally used to describe the sum of all the processes in which water is converted from the land surface to the water vapor into the atmosphere, including all kinds of free water evaporation, soil evaporation, and vegetation transpiration (Sun 2007).

At present, global climatic changes have become a major problem threatening the survival of human beings. The WUE of plants is dominantly driven by climate (Sheng et al. 2011), and the changes of meteorological factors on carbon and water fluxes could affect WUE (Zhang et al. 2014). However, The correlations between WUE and temperature and precipitation were different in different regions. Yu et al. (2008) reported that air temperature and precipitation increased while WUE of forest ecosystems decreased from north to south in Eastern China. Niu et al. (2011) revealed that, in Northern China, climate warming could decrease the ecosystem WUE, while the ecosystem WUE increased with increasing precipitation. Zhang et al. (2016) simulated the temporal and spatial changes of WUE in the alpine area of Southwestern China by using a process-based ecosystem model during 1954–2010 and found that there were significant negative correlations between the WUE and temperature, and significant positive correlations were discovered between annual WUE and annual precipitation in 34.1% of that area. Xiao et al. (2013) revealed that higher WUE corresponded to a higher temperature and precipitation in China. Zhang et al. (2014) found that the climatic changes negatively influenced WUE in the northwest, north, and east of East Asia, which could reduce WUE in most regions of East Asia. Meanwhile, the correlation between WUE and temperature was highly positive in the Tibet Plateau and highly negative in the subtropical zones, while WUE showed high positive correlations with precipitation in wet temperate zones (Zhang et al. 2012).

Human activities and climatic change are two main factors of the carbon cycle of terrestrial ecosystems (Chen et al. 2014). Therefore, anthropogenic activities could influence WUE as well (Jiang et al. 2007). Chen et al. (2014) calculated the human-induced NPP over the Qinghai–Tibet plateau from 1982 to 2011 and revealed that the impact of human activities in the latter period was stronger than that in the former 20 years. Spatio-temporal Pattern of Net Primary Productivity in Hengduan Mountains area, China: Impacts of Climate Change andHuman Activities. Anthropogenic activities like irrigation or reservoir impoundment could also influence regional ET (Pan et al. 2017). Contributions of climate change and human activities to ET and GPP trends over North China Plain from 2000 to 2014, Chen et al. (2017b) pointed out that human activities were the main factor affecting the long-term trends of ET in the North China Plain. Zou et al. (2017) examined the ET in the Heihe from 1984 to 2014 by using the remote sensing data with the Soil and Water Assessment Tool and discovered that the influences of human activities on ET were dramatically greater than that of climatic change. WUE is generally defined as the ratio of NPP to ET. Therefore, the changes of NPP and ET driven by human activities could result in the variations of WUE.

Recently, several models have been used to estimate NPP and ET. Chen et al. (2017a) simulated the NPP in Hengduan Mountains of China by using the Carnegie-Ames-Stanford Approach (CASA) model. Meanwhile, an improved Shuttleworth–Wallace (S-W) model, namely SWH model, was developed to calculate ET by using meteorological and remote sensing data (Hu et al. 2017). Lund-Potsdam-Jena (LPJ) Dynamic Global Vegetation Model is a model that could simultaneously reveal the dynamic changes of NPP and ET under different climate scenarios (Babst et al. 2013). However, since the primary driving factor of LPJ model is climate data, it could only reflect the changes of WUE under the pure climate changes. Therefore, observational proxies like normalized difference vegetation index (NDVI) should be considered to ensure the reliability of the results (Rafique et al. 2016). NDVI is a common graphical indicator, which could monitor the variety of vegetation by using remote sensing measurements (Asrar et al. 1984). Therefore, NDVI could be used as an observational proxy to study the varieties of NPP. Many researchers have discovered that accumulated NDVI is closely linked to NPP (Fensholt and Rasmussen

Table 1 Introduction to three forestry regions of China

Vegetation form	Northeast region Natural forest	Southwest region Natural forest	Southeast region Artificial forest
Longitude	120.25 ~ 133.25° E	91.75 ~ 109.25° E	104.25 ~ 121.25° E
Latitude	39.75 ~ 53.25° N	21.75 ~ 33.75° N	18.75 ~ 32.75° N
Annual mean temperature	− 6.9 ~ 9.3 °C	-5.6 ~ 21.7 °C	6.8 ~ 24.2 °C
Annual mean precipitation	407.7 ~ 1002.2 mm	372.1 ~ 2220.4 mm	798.0 ~ 2459.6 mm
Total forest area	435,539 km^2	479,861 km^2	810,588 km^2
Total forest stock [1]	3.88 billion m^3	5.56 billion m^3	3.71 billion m^3
Dominant species	*Pinus koraiensis, larch, spruce, fir, red pine et al.*	*Spruce, fir, oak, yunnan pine, teak, red sandalwood et al.*	*Chinese fir, masson pine, cinnamon, eucalyptus, camphor tree, bamboo et al.*

[1] The total forest stock data came from the sixth national forest census

2011; Holm et al. 2003). Therefore, WUE_{NDVI}, which was calculated by accumulated NDVI and ET, could be used to reflect the influences of climatic changes and human activities on WUE.

China is a vast country with a wide variety of trees. According to incomplete statistics, China's total forest stock is 15.14 billion m^3 in 2017, accounting for around 2.5% of the world's total forest stock. The three traditional forestry regions of China (the northeast, southwest, and southeast forest regions) provide the great mass of forest resources of China. Therefore, they are important to the carbon and water cycle of China. The northeast and southwest forest regions are natural forest regions, and the southeast forest region belongs to the artificial forest region. Although there were many studies on the responses of WUE to climate change, few studies focused on the response of forest WUE to climate change and human activities. Therefore, the purposes of this study were (1) to disclose the temporal and spatial distribution of forest WUE in three forestry regions of China from 1961 to 2019 and (2) to evaluate the impact of climatic changes and human activities on the forest WUE in the three regions, and then expound the causes of the forest WUE varieties at the regional scale. The conclusions of this paper were of great importance to the forest water cycle and carbon cycle of natural and artificial forest regions and are expected to promote the comprehensive utilization of timber resources.

2 Materials and methods

2.1 Study area and data

The three forestry regions of China are the northeast, southwest, and southeast forest regions (as shown in Fig. 1 and Table 1). The forests of our country are basically concentrated there (Fig. 1a). The northeast forest region is a natural forest region, which includes the Da Hinggan Mountains, Xiao Hinggan Mountains, and Changbai Mountain. The northeast forest region is located in northernmost China, closes to the cold zone. The northeast forest area is the only area with extensive larch forest in China, and the forest stock there is more than 1/4 of the total in China. The Southwest forest region is another natural forest region. This area includes the Hengduan Mountains at the junction of Sichuan, Yunnan, and Tibet, along with the south slope of the Himalayas in southeastern Tibet. The southwest forest region is a mountainous forest, so the climate there changes with the height of mountains. In this region, there are evergreen broadleaf forests below the mountains and deciduous broadleaf forests on the mountainsides. Needleleaf forests are on the top of the mountains there. The southeast forest region (or south forest region) belongs to the artificial forest region, which contains Qinling Mountains, south of Huai River, and a vast area in the east of the Yunnan-Guizhou Plateau. The climate there is warm and damp. The southeast forest area has many kinds of trees, including the unique bamboo in China.

Temperature, precipitation, NPP, and ET from 1961 to 2019 in the forest ecosystems of three forestry regions of China were used in this study. Accumulated NDVI during the period of 1982-2013 in the study areas were used as well. Missing data were interpolated by using the inverse distance weighted (IDW) method. The temperature and precipitation data during 1961–2019 were from National Meteorological Information Center (http://data.cma.cn/site/index.html). The NPP and ET data sets from 1961 to 2019 were simulated by LPJ global vegetation dynamics model. The spatial resolution of temperature, precipitation, NPP, and ET was 0.5° × 0.5°. The WUE data was calculated by NPP and ET.

The NDVI dataset used to validate the results of LPJ model came from Global Inventory Modeling and Mapping Studies (GIMMS) group, https://ecocast.arc.

nasa.gov/data/pub/gimms/3 g.v1/) which has been calibrated for cloud test and sensor-shift. The NDVI data was from 1982 to 2013 and at a spatial resolution of 8 km × 8 km. The WUE_{NDVI} was computed by accumulated NDVI and ET. The ET data simulated by Variable Infiltration Capacity (VIC) large-scale distributed hydrological model during 1982–2013 was used to validate the value of ET estimated by LPJ model.

The land use and land cover change (LUCC) data set of 1980 and 2018 was provided by Data Center for Resources and Environmental Sciences, Chinese Academy of Sciences (RESDC) (http://www.resdc.cn). The resolution of the LUCC data was 1 km. The national land use/cover data could be divided into six classifications: forests, cultivated land, grasslands, waters, construction land, and unused land (Fig. 1b).

2.2 Methodology

LPJ model is a model coupled with terrestrial vegetation dynamics and the carbon-water cycle, which is based on the

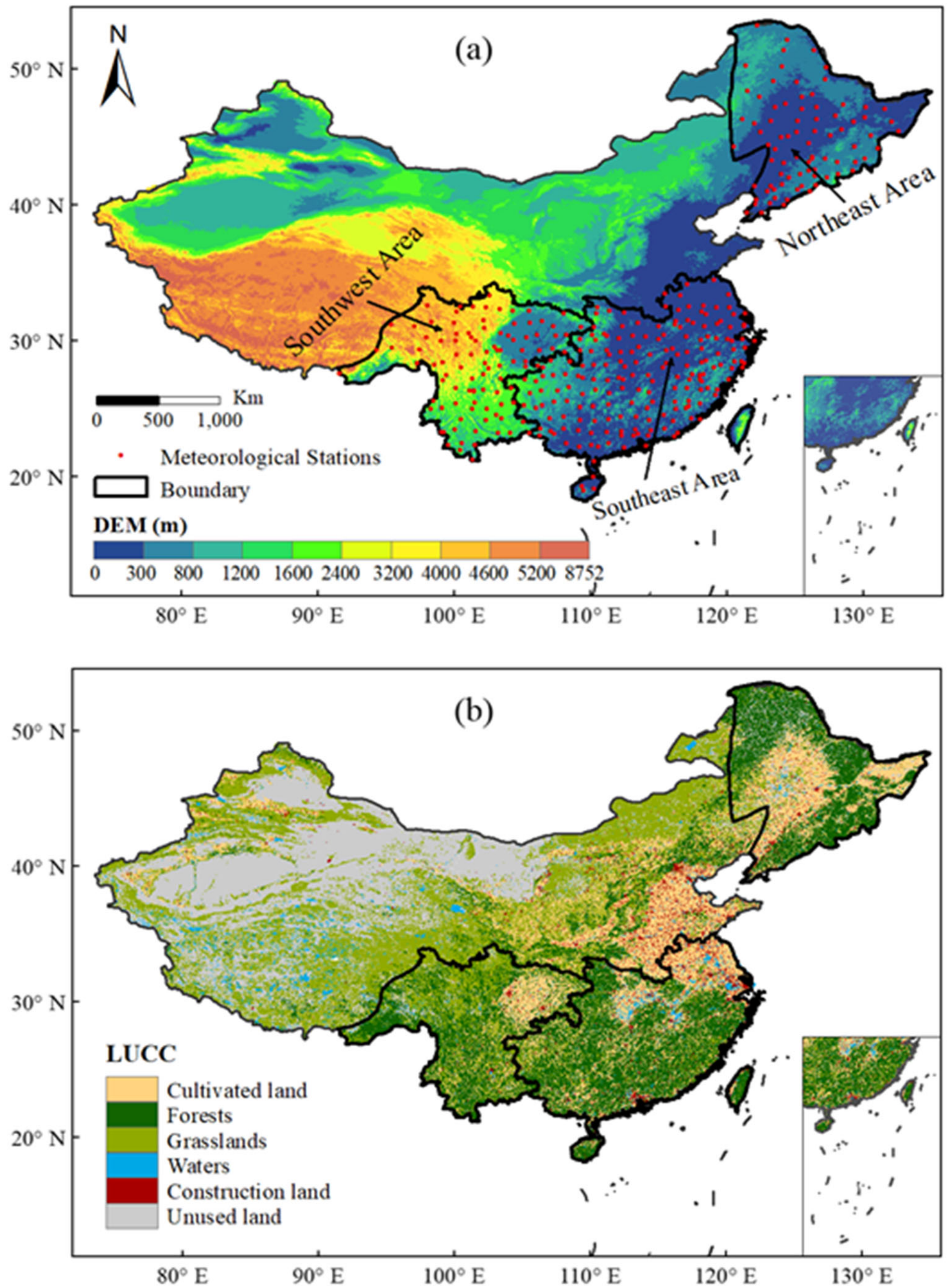

Fig. 1 **a** Study area maps and location of the observed meteorological stations, and **b** the land use and land cover change (LUCC) classification in 2018

framework of the BIOME series model (Sun et al. 2007). The input data of LPJ model includes monthly mean temperature, monthly precipitation, monthly cloud cover, annual CO_2 concentration, soil texture, and monthly wet days. Ten plant functional types (PFTs) are used in LPJ model to generalize vegetation types. The NPP of each PFT uses the following formula:

$$NPP = \mathrm{Max}[0.75 \times (GPP - R_m), 0] \tag{1}$$

where GPP is gross primary productivity, gC·m^{-2}a^{-1}; R_m is the carbon content to maintain the breathing you need; and 0.25 represents that 25% of the $GPP - R_m$ is consumed for the growth of vegetation.

LPJ model simply uses a two-layer tank model to describe the water cycle process. Take the rate of equilibrium evaporation (E_q, which is calculated by Priestley-Taylor formula), and multiply by the coefficient of Priestley-Taylor formula (α, the value of the model is 1.32). The value we got is potential evaporation. Actual evapotranspiration includes vegetation transpiration (EP), vegetation interception (EI), and bare-soil evaporation (ES). The water budget of the upper and lower layers is calculated by the following equations:

$$\Delta W_1 = P + M - ES - EI - \beta_1 \times EP - R_1 - Perc_1 \tag{2}$$

$$\Delta W_2 = Perc_1 - \beta_2 \times EP - R_2 - Perc_2 \tag{3}$$

where ΔW_1 and ΔW_2 represent the variety of soil moisture content in the upper and lower layers, mm·d^{-1}; β_1 and β_2 are the ratios of water consumed by the root system for vegetation transpiration in the upper and lower layers; R_1 and R_2 represent runoff producing of surface and underground, mm·d^{-1}; $Perc_1$ and $Perc_2$ represent the soil infiltration quantity in the upper and lower layers, mm·d^{-1}; P is precipitation, mm·d^{-1}; M means snow melting volume, mm·d^{-1}.

EI is the function of E_q, which is calculated by the following formula:

$$EI = E_q \times \alpha \times f_{\mathrm{wet}} \tag{4}$$

where f_{wet} represents the ratio of canopy wetness of each PFT during the daytime. The remaining 1-f_{wet} canopy was used to reckon EP.

EP is vegetation water demand (D) and the minimum value of vegetation water supply (S) under adequate water supply circumstances. The computational formula of EP is:

$$EP = \mathrm{Min}[S, D] \times f_v \tag{5}$$

$$S = E_{\max} \times W_r \tag{6}$$

$$D = E_q \times \alpha_{\max} \times (1 - f_{\mathrm{wet}}) / \left(1 + \frac{g_m}{g_{\mathrm{pot}}}\right) \tag{7}$$

where $E_{\max}$ is the maximum transpiration rate of each PFT, value ranges from 5 to 7 mm·d^{-1}; W_r the soil moisture content that can be used by vegetation root system; α_{max} is the maximum Priestley-Taylor coefficient, value is 1.391; g_m is conversion conductivity, value is 3.26 mm·s^{-1}; g_{pot} represents canopy potential conductivity, mm·s^{-1}; f_v means vegetation coverage.

ES only occurs in the surface 20 cm soil horizon of bare land (1-f_{wet}), it is positively correlated to the surface soil moisture content W_{r20}. ES is defined as:

$$ES = E_q \times \alpha \times wr_{20} \times (1 - f_v) \tag{8}$$

WUE is generally defined as the ratio of NPP to ET.

$$WUE = \frac{NPP}{ET} \tag{9}$$

WUE_{NDVI} is generally defined as the ratio of accumulated NDVI to ET.

$$WUE_{NDVI} = \frac{\sum_1^i NDVI_i}{ET} \tag{10}$$

The sensitivity of WUE to temperature and precipitation is analyzed by changing the input temperature and precipitation data of LPJ model. The relative variations of temperature were − 2 °C, − 1.5 °C, − 1 °C, − 0.5 °C, and 0.5 °C, 1 °C, 1.5 °C, 2 °C, and the relative changes of precipitation were − 25%, − 15%, − 5%, and 5%, 15%, 25%.

3 Results

3.1 The LPJ model calibration and WUE calculation

Many researchers discovered that accumulated NDVI is closely linked to NPP (Fensholt and Rasmussen 2011; Holm et al. 2003), so we used accumulated NDVI to evaluate the reliability of NPP data. Figure 2a1–a3and Fig. 2b1–b3showed the distribution of annual mean NPP and accumulated NDVI in the forest ecosystem of three forestry regions of China from 1982 to 2013. The spatial pattern of annual mean NPP and accumulated NDVI was similar in the three major forest regions, especially in the west and south edge of the southwest forest region (Fig. 2a2, b2), along with the southern and southeastern part of the southeast forest area (Fig. 2a3, b3). However, in the northeast forest region, the highest NPP (> 575 gC·m^{-2}·a^{-1}) occurred in the southwestern area, while the highest NDVI (> 7.5) appeared in the east and southeast. Generally, the NPP and NDVI were the lowest in the northeast forest region, while relatively high in the southeast forest region. Both the NPP and NDVI were quite high in Hainan province. The spatial distribution of annual mean forest ET of LPJ and VIC models in three forestry regions of China during 1982–2013 was shown in Fig. 2c1–c3and Fig. 2d1–d3. It was clear that the ET driven by LPJ model was significantly higher than that derived by VIC model in the southeast of the

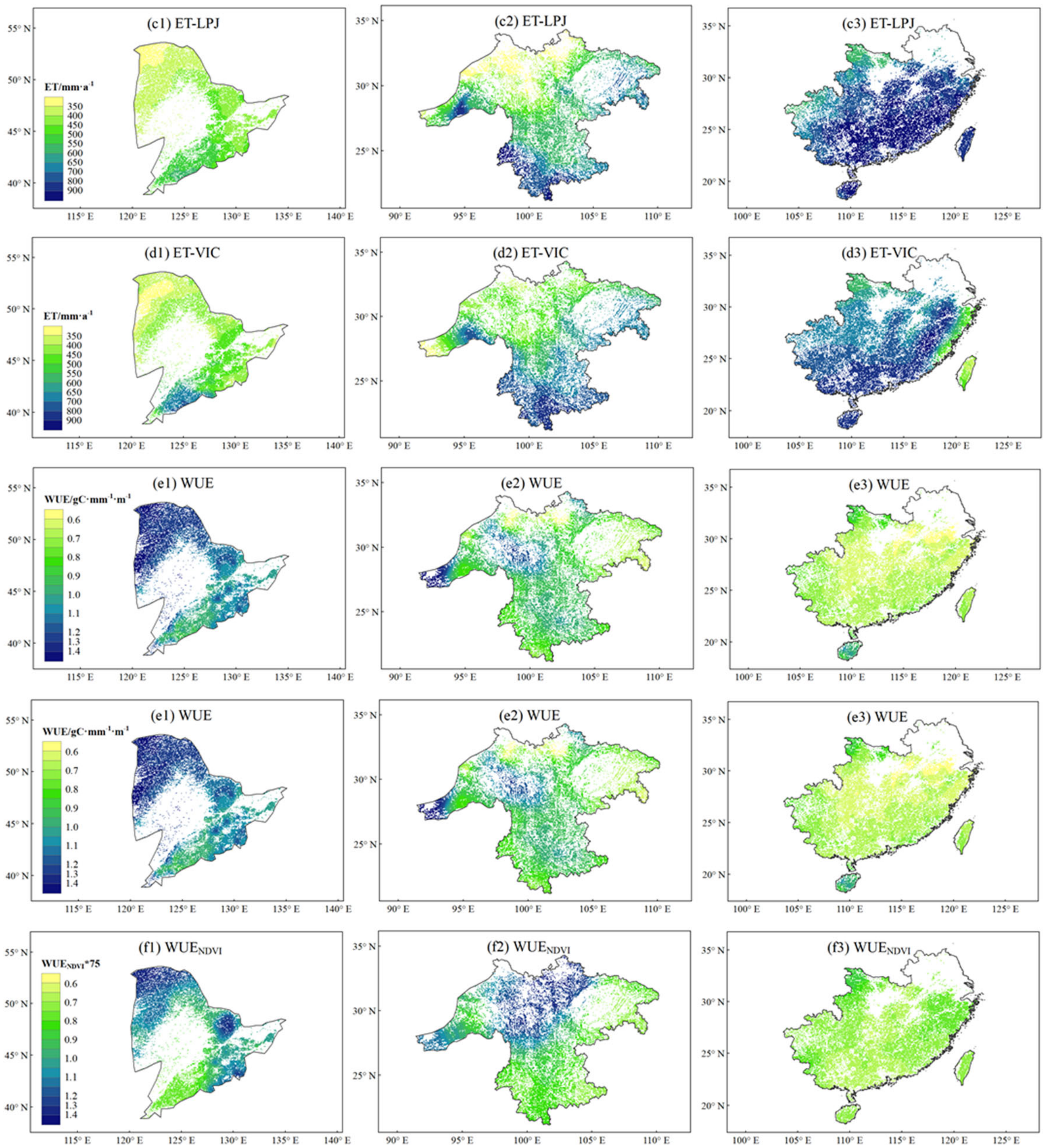

Fig. 2 Spatial distribution of **a1**–**a3** annual mean forest NPP, **b1**–**b3** accumulated NDVI, annual mean forest ET simulated by **c1**–**c3** LPJ and **d1**–**d3** VIC models, annual mean forest **e1**–**e3** WUE, and **f1**–**f3** WUE_{NDVI} in three forestry regions of China during 1982–2013

southeast forest region (Fig. 2c3, d3). Overall, the ET estimated by the two models over the whole three forestry regions of China presented decreasing trends from the southeast (> 900 $mm{\cdot}a^{-1}$) to the northwest (< 350 $mm{\cdot}a^{-1}$). The ET in the artificial forest region was much higher than that in the two natural forest regions. The spatial distribution of annual mean forest WUE and WUE_{NDVI} in three forestry regions of China during 1982-2013 was analyzed as well (Fig. 2e1–e3 and Fig. 2f1–f3). WUE_{NDVI} could be defined as the ratio of accumulated NDVI to ET, which could reflect the influences of climatic changes and human activities on WUE. Generally, WUE and WUE_{NDVI} showed similar spatial patterns in three forestry regions of China. However, the highest WUE (> 1.4 $gC{\cdot}mm^{-1}{\cdot}m^{-2}$) occurred in the westernmost point of the southwest forest region, and the northwest of the northeast forest region (Fig. 2e1), while the highest WUE_{NDVI} (0.0187) appeared in the northwest and east of the northeast forest region, along with the north of the southwest forest region (Fig. 2f1, f2). Overall, the forest WUE and WUE_{NDVI} both decreased from northwest to southeast over the study region.

As was shown in Fig. 3a–c, the patterns of annual mean forest NPP and accumulated NDVI were quite different in most years. This was due to the NPP which was driven by LPJ model did not consider the impacts of human activities. Generally, human

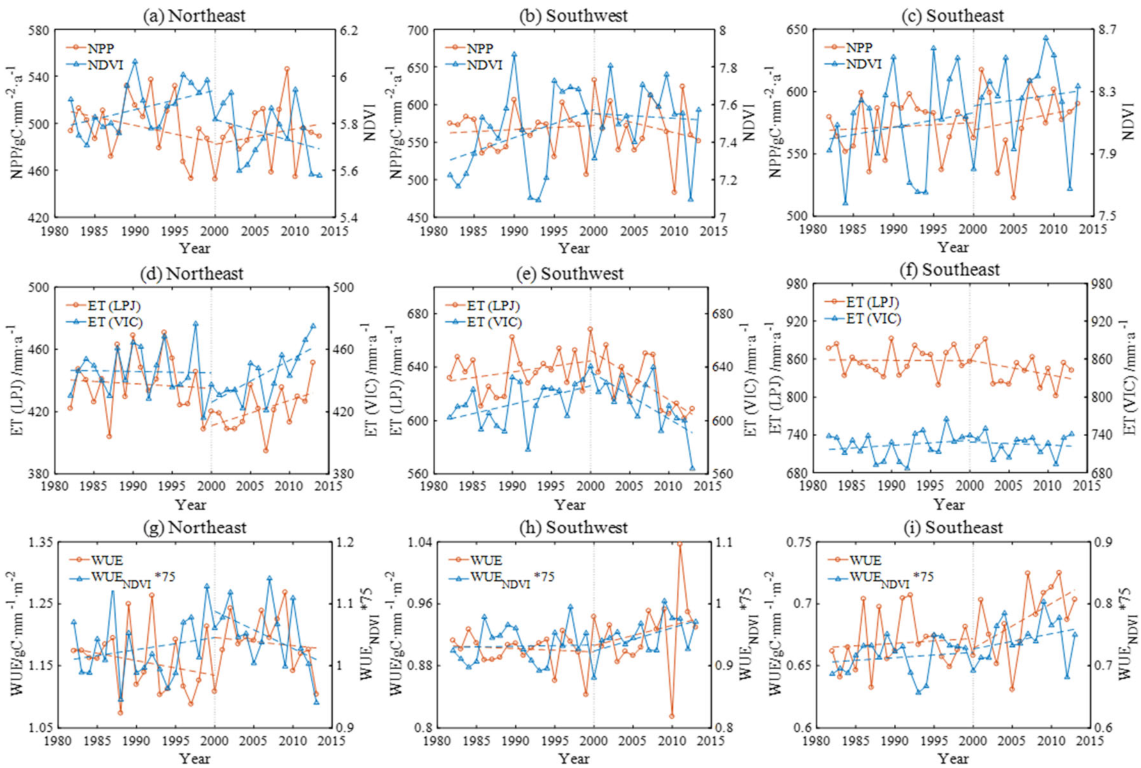

Fig. 3 The **a**–**c** annual mean forest NPP and accumulated NDVI, **d**–**f** annual mean forest ET simulated by LPJ and VIC models, **g**–**i** annual mean forest WUE and WUE_{NDVI} in three forestry regions of China during 1982–2013

activities could increase the vegetation in the northeast forest region from 1982 to 1999. However, during 2000–2013, human activities have resulted in vegetation degradation there (Fig. 3a). It could be seen that the annual mean forest ET simulated by LPJ and VIC models showed similar performance in three forestry regions of China from 1982 to 2013 (Fig. 3d–f). As was shown in Fig. 3d, ET driven by the LPJ model was slightly underestimated in the northeast forest region. However, the LPJ model significantly overestimated the ET in the southwest and southeast forest regions, especially in the southeast forest region (Fig. 3e, f). This phenomenon was similar to the results in Fig. 2c 3, d3. In the northeast forest region, forest ET decreased during 1982–1999, while increased sharply from 2000 to 2013 (Fig. 3d). The forest ET in the southwest exhibited an opposite trend (Fig. 3e). The evolution trend of forest ET was relatively stable in the southeast forest region (Fig. 3f). Generally, the LPJ model performed well in simulating the NPP and ET (Fig. 3a–f). WUE_{NDVI} could reflect the combined impact of climatic changes and human activities on WUE. The annual mean forest WUE and WUE_{NDVI} during 1982–2013 in three forestry regions of China were presented in Fig. 3g–i. It could be seen that the WUE and WUE_{NDVI} in the two natural forest regions were higher than that in the artificial forest region, especially in the northeast forest region. This might be due to the relatively high ET caused by the good hydrothermal condition in the southeast forest region. Overall, in the southwest and southeast forest regions, the changing trend of WUE and WUE_{NDVI} were not significant during 1982–1999, while increased significantly after 2000 (Fig. 3h, i). In the northeast forest region before 2000, the forest WUE showed a decreasing trend, whereas the forest WUE_{NDVI} presented an increasing trend.

3.2 The spatial and temporal distribution of the forest WUE

Figure 4 and Fig. 5 were applied to indicate the spatial and temporal distribution of WUE from 1961 to 2019. As was presented in Fig. 4a,b, the highest WUE (> 1.4 $gC \cdot mm^{-1} \cdot m^{-2}$) occurred in the western of the southwest forest region and the northwest of the northeast forest region. As for the southeast forest region, the forest WUE was all under 1.1 $gC \cdot mm^{-1} \cdot m^{-2}$ (Fig. 4c). Overall, the forest WUE decreased from northwest to southeast over the whole three forestry regions of China. The temporal distribution of forest WUE during 1961–2019 in three forestry regions of China were indicated in Fig. 5. It could be seen that the WUE in the northeast forest region was the highest, and the WUE in the southeast forest region was the lowest. Overall, the forest WUE in all forest regions showed increasing trends from 1961 to 2019, especially in the southwest forest region.

Changing trends of annual mean forest WUE and WUE_{NDVI} in three forestry regions of China during the periods of 1961–1999, 2000–2019, and 1961–2019 were shown in Fig. 6. From 1961 to 1999, the forest WUE presented

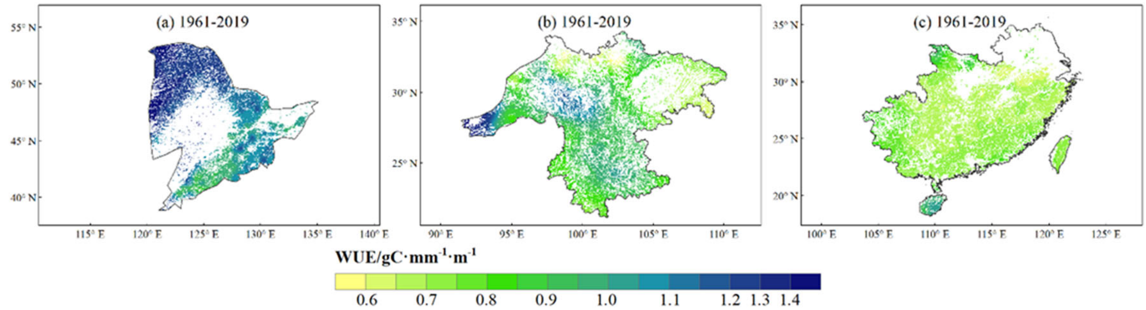

Fig. 4 Spatial distribution of annual mean forest WUE in three forestry regions of China during 1961–2019

increasing trends in most parts of the three major forest regions. The WUE even increased significantly in the east of the northeast forest region, portions of the north of southwest forest region, and west of the southeast forest region. The areas with WUE decreasing trends were concentrated in the north of the northeast forest region, the west and south of the southwest forest region, along the north and south of the southeast forest region. More areas presented WUE decreasing trends from 2000 to 2019 (Fig. 6d–f). In the southeast forest region, even half of the forests showed a decreasing trend in WUE (Fig. 6f). Look from the whole period of 1961–2019, the forest WUE increased in almost all the study areas (Fig. 6g–i). However, the WUE of the west of the southwest forest region still presented a declining trend from 1961 to 2019 (Fig. 6h).

The northeast and southwest forest regions are natural forest regions, while the southeast forest region is an artificial one. The longitude distributions of annual mean WUE in the forest ecosystem of the three forest regions during 1961–1999 and 2000–2019 were presented in Fig. 7a. It could be seen that the variations of WUE with longitude were fluctuant sharply in the southwest forest region, while very gentle in the northeast and southeast forest regions. It could be due to the complex terrain in the southwest forest region (Fig. 1a). The forest WUE decreased from 91.75° E to 109.25° E. However, the decrease in the southeast forest region was not significant. In the northeast forest region which is located in the high latitude region, the forest WUE decreased markedly with the increase of longitude as well. The latitude distributions of annual mean WUE in the forest ecosystem of three forestry regions of China before and after 2000 were analyzed in Fig. 7b. It could be seen that the WUE of the southwest decreased from 27.25° N to 32.75° N, while increased sharply from 32.75° N to 33.75° N due to the increase of elevation (Fig. 1a). However, from 30.25° N to 32.75° N, the forest WUE in the artificial forest region increased with elevation. In the southeast forest region, the highest WUE occurred in Hainan province. Overall, the WUE increased with the increase of latitude. The WUE in the northeast forest region was higher than that in the southwest and southeast forest regions. In addition, the WUE in the artificial forest region was the lowest. The annual mean WUE after 2000 was slightly higher than that before 2000.

3.3 The impacts of climatic change and human activities on the forest WUE

The forest WUE could be affected by climate changes. Therefore, the sensitivity of WUE to temperature and precipitation was analyzed in Fig. 8. The relative variations of

Fig. 5 The annual mean forest WUE in three forestry regions of China during 1961–2019

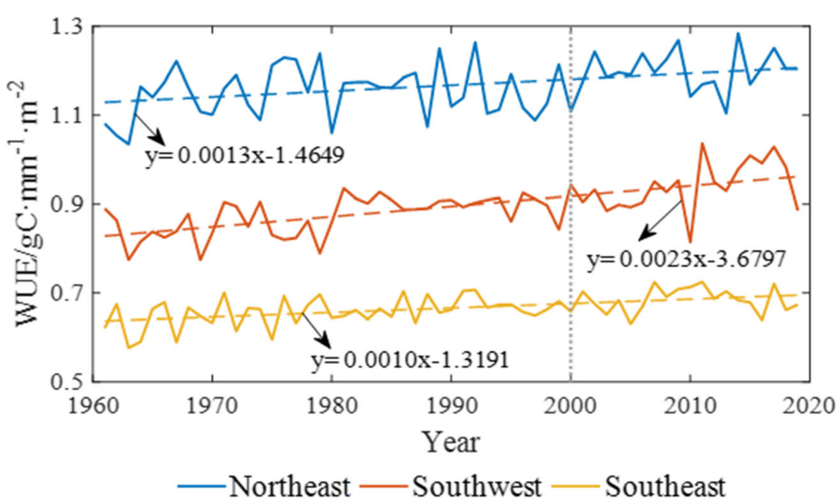

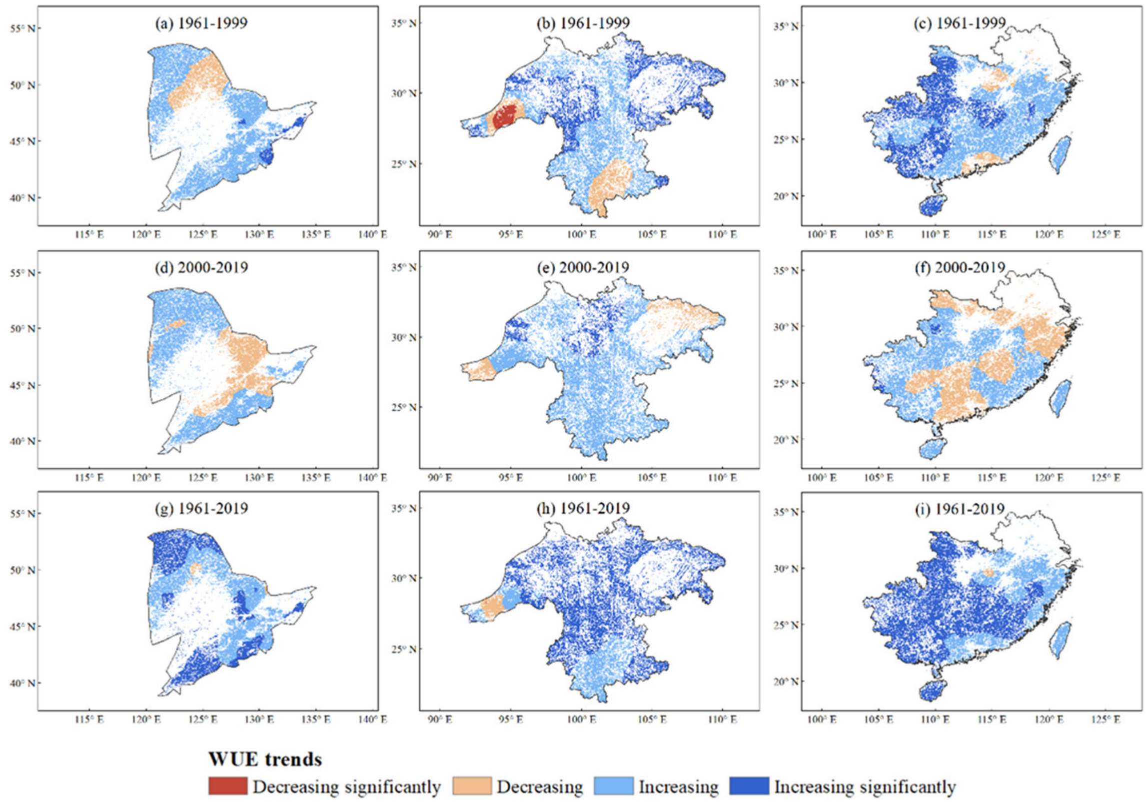

Fig. 6 Changing trends of annual mean forest WUE in three forestry regions of China during the period of **a**–**c** 1961-1999, **d**–**f** 2000-2019, and **g**–**i** 1961-2019

temperature were − 2 °C, − 1.5 °C, − 1 °C, − 0.5 °C, and 0.5 °C, 1 °C, 1.5 °C, 2 °C (Fig. 8a). It could be found that, generally, the WUE was negatively correlated with the temperature in the northeast and southeast forest regions while it was positively correlated with the temperature in the southwest forest region. In the northeast forest region, the relative changes in WUE decreased significantly with the increase of temperature from − 2 °C to 1 °C. Then, the forest WUE began to be positively correlated with temperature from 1.5 °C. In the southwest forest region, when the temperature rose by 1 °C, the increase rate of WUE slowed down significantly. The WUE of the southeast forest area did not show obvious variety with the change of temperature, especially when the temperature varied from − 1 °C to 0 °C. It could be due to the high temperature and adequate heat there. Overall, the WUE was not sensitive to the increase of temperature in the three forestry regions of China. The relative changes of precipitation were − 25%, − 15%, − 5%, and 5%, 15%, 25% (Fig. 8b). As was shown in Fig. 8b, the forest WUE was negatively correlated with the precipitation in all three forestry regions of China. Overall, the WUE was very sensitive to the changes in precipitation over the three major forest regions, especially to the

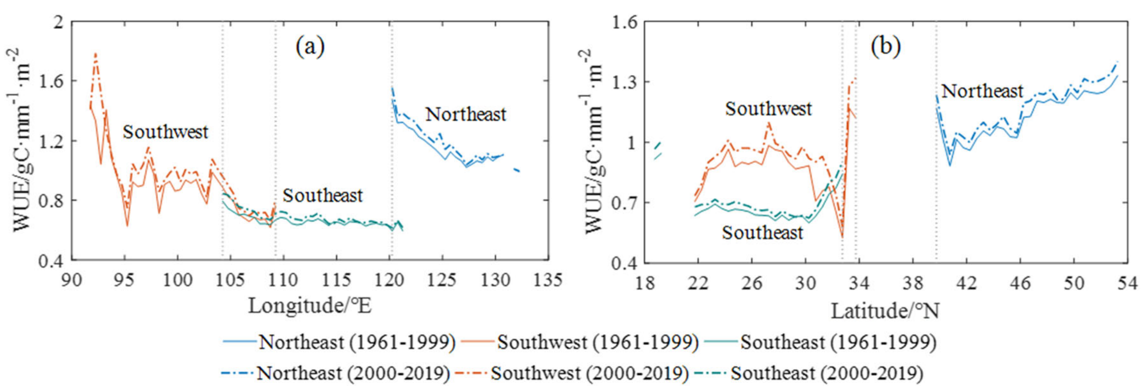

Fig. 7 The **a** longitude and **b** latitude distribution of annual mean WUE in the forest ecosystem of three forestry regions of China during 1961–1999 and 2000–2019

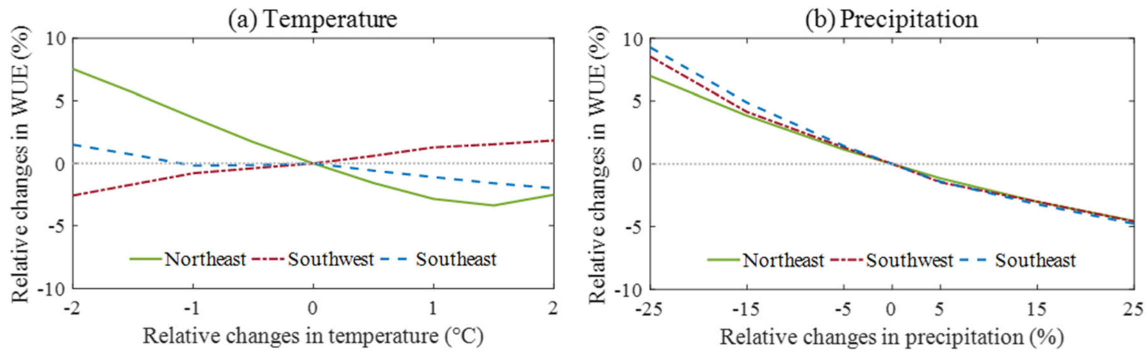

Fig. 8 The sensitivity of WUE to **a** temperature and **b** precipitation in the forest ecosystem of three forestry regions of China during 1961–2019

decrease of precipitation. The sensitivity of WUE to precipitation decrease was highest in the southeast forest region and lowest in the northeast forest region. As for the increase of precipitation, the relative changes in WUE were very similar in three forestry regions of China.

As was shown in Fig. 3, from 1982 to 1999, only the northeast forest region showed a significant downward trend in NPP, ET, and WUE. This might be related to the high latitude in the northeast forest region. The annual mean temperature Mann-Kendall statistics in forest ecosystem of three forestry regions of China was revealed in Fig. 9. It could be discovered that the temperature in the northeast forest region had an abrupt change in 1989 (Fig. 9a). In fact, the temperature there increased from 1981 and increased significantly after 1990. The increase in temperature could decrease the forest WUE there. However, the abrupt change points of the southwest and southeast forest regions were between 2001 and 2002 (Fig. 9b, c), and then the temperature in the two forest regions increased sharply.

The forest WUE could also be affected by human activities. In fact, human activities and climatic changes could interact with each other. As previously mentioned, the variations of WUE and WUE_{NDVI} were quite different in the three forest regions. As was shown in Fig. 2e2, f2, in the southwest forest region, the highest WUE was in the westernmost point, while the WUE_{NDVI} in the north was higher than that in other areas. In the northeast forest region before 2000, human activities have increased the WUE_{NDVI} (Fig. 2g). There were five key national ecological projects in three forestry regions of China (Table 2). 3-North Shelter Forest Program, which covered parts of the northeast region, was initiated in 1978. In the past 40 years, the area of the forest there has increased from 206,000 km^2 to 591,000 km^2. Coastal Shelterbelt Project started in 1988. Coastal shelterbelt refers to coastal forests, trees, and shrubs with the main purpose of protection. By 2015, the forest coverage in the coastal regions has reached 37.3%. The Yangtze River Shelter Forest, which planned to protect the water resources of the Yangtze River, began in 1989. The forest area and accumulation of this project have been effectively increased, and the ecological service function of the system has been significantly improved. Returning Farmland to Forest was the largest ecological project in the world. This project started in 1999 and had obviously improved the ecological condition. Natural Forest Resources Protection project was initiated in 2000. The main goal of this project is to solve the problems of natural forest recuperation and recovery and finally realize the coordinated development of forest resources, economy, and society. The area of three forestry regions of China covered by the Natural Forest Resources Protection project was the largest among the five ecological projects.

In this paper, the land use transition matrix in three forestry regions of China from 1980 to 2018 was analyzed in Tables 3, 4, and 5. As was shown in Table 3, the forest area in the northeast forest region decreased by 5,075 km^2 (1.42%), while increased by 83,841 km^2 (19.25%) from 1980 to 2018. Thereinto, 38,946 km^2 grasslands and 33,236 km^2 cultivated land have been converted to forests. Meanwhile, 2130 km^2 and 1657 km^2 forests

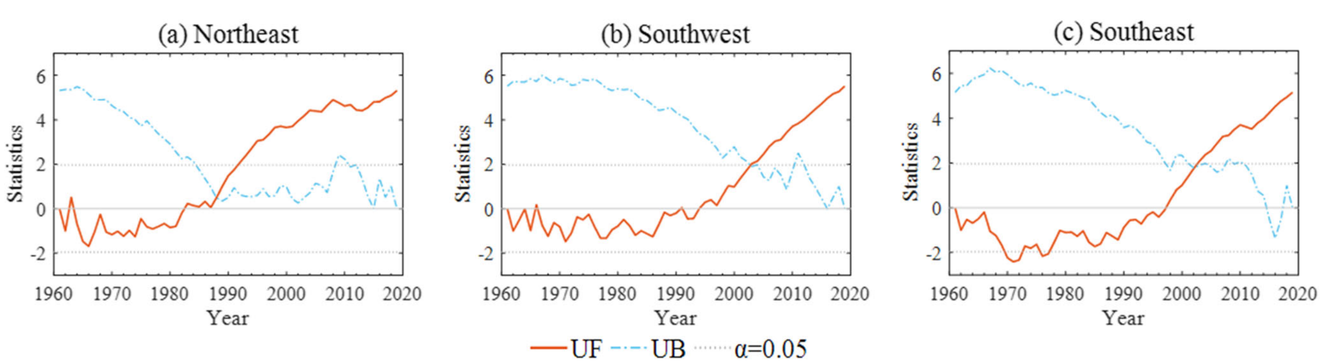

Fig. 9 Annual mean temperature Mann-Kendall statistics in forest ecosystem of three forestry regions of China during 1961–2019

Table 2 Characteristics of the forest ecological projects in three forestry regions of China

Code	Ecological projects	Start time	Distribution
1	3-North Shelter Forest Program	1978	Northeast region
2	Coastal Shelterbelt Project	1988	Three regions
3	Yangtze River Shelter Forest	1989	Southwest and southeast regions
4	Returning Farmland to Forest	1999	Three regions
5	Natural Forest Resources Protection	2000	Three regions

have been converted to cultivated land and unused land, respectively. Only 1022 km^2 forests have been converted to grasslands. When it came to the southwest forest region, the area of forest decreased by 29,878 km^2 (8.20%), of which 17,478 km^2 was converted to grasslands and 11,110 km^2 to cultivated land (Table 4). In the meantime, the forest area increased by 145,468 km^2 (30.31%). The greatest contributors were grasslands (84,686 km^2) and cultivated land (46,730 km^2). From 1980 to 2018, the increase in the forest area of the artificial forest region was 170,638 km^2 (21.05%), while increased by 14,663 km^2 (2.24%) (Table 5). The area converted from forests to cultivated land was 9,617 km^2, and the area converted from forests to grasslands area was 3656 km^2. Around 113,580 km^2 cultivated land and 46,774 km^2 grasslands have been converted to forests. Generally, in the northeast, southwest, and southeast forest regions, the area of forests that converted into unused land was 1657 km^2, 581 km^2, and 13 km^2, respectively. Therefore, the forest fire on May 6, 1987, has had a certain influence on the northeast forest region. This forest fire was the most serious one since 1949 and could destroy the forest of the northeast forest region. Overall, the forest area of three forest regions increased by 145,468 km^2 from 1980 to 2018. The greatest contributor was cultivated land (193,546 km^2). It indicated that the Returning Farmland to Forest project was being carried out steadily. Meanwhile, the total area of forest decreased by 49,616 km^2. Therefore, the net increase of forest area in the three forest regions was 350,331km^2 (78,766km^2 in the northeast forest region, 115,590km^2 in the southwest forest region, and 155,975km^2 in the southeast forest region). It meant that the implementation of the ecological projects could alleviate the degradation of forests.

4 Discussion

WUE, which defined as the ratio of NPP to ET, is a critical link between the carbon cycle and the water cycle in forest ecosystems and is important for the productivity and health of plants under future climatic changes (Xiao et al. 2004; Xu and Hsiao 2004; Niu et al. 2011). The WUE calculated by NPP and ET of the LPJ model was used in this paper. In three forestry regions of China, the LPJ model performed well in simulating the NPP and ET. However, Rafique et al. (2016) proposed that observational proxies like NDVI should be considered to ensure the reliability of the results. This paper evaluated the annual mean forest NPP and accumulated NDVI and discovered that they presented a similar pattern in the study region, which meant that there was a close relationship between accumulated NDVI and NPP (Fensholt and Rasmussen 2011; Holm et al. 2003). Therefore, the NPP could be replaced by the accumulated NDVI in the calculation of WUE (Chang et al. 2018). Overall, WUE and WUE_{NDVI} showed similar spatial patterns in three forestry regions of China. Both the forest WUE and WUE_{NDVI} decreased from northwest to southeast over the whole three forestry regions of China, which were consistent with the conclusions of Yu et al. (2008). However, the highest WUE (> 1.4 $gC{\cdot}mm^{-1}{\cdot}m^{-2}$) occurred in the western of the southwest forest region and the

Table 3 The land use transition matrix in the northeast forest region (area, unit: km^2)

		2018						
		Cultivated land	Forests	Grasslands	Waters	Construction land	Unused land	Decrease
1980	Cultivated land	556	33,236	41	19	60	63	33,419
	Forests	2130	351,698	1022	152	114	1657	5075
	Grasslands	236	38,946	228	15	15	479	39,691
	Waters	13	1987	4	24	0	10	2014
	Construction land	33	2282	1	1	2	2	2319
	Unused land	86	7390	24	4	1	116	7505
	Increase	2498	83,841	1092	191	190	2211	

Table 4 The land use transition matrix in the southwest forest region (area, unit: km^2)

		2018						
		Cultivated land	Forests	Grasslands	Waters	Construction land	Unused land	Decrease
1980	Cultivated land	6073	46,730	1596	88	115	7	48,536
	Forests	11,110	334,393	17,478	482	227	581	29,878
	Grasslands	2053	84,686	10,288	92	48	477	87,356
	Waters	67	2404	140	59	2	48	2661
	Construction land	50	315	14	0	5	0	379
	Unused land	10	11,333	704	33	0	531	12,080
	Increase	13,290	145,468	19,932	695	392	1113	

northwest of the northeast forest region, but the highest WUE_{NDVI} (0.0187) appeared in the northwest and east of the northeast forest region, along with the north of the southwest forest region. Generally, the WUE and WUE_{NDVI} in the two natural forest regions were higher than that in the artificial forest region, and the WUE and WUE_{NDVI} in the northeast forest region were the highest. The spatial variation of WUE was much more gentle in the artificial forest region. The WUE of the southwest forest region increased with the increase of elevation, while the forest WUE in the southeast forest region increased with the decrease of elevation.

Recently, global climatic change has become a major problem threatening the survival of human beings. Climate changes could even result in the sixth mass extinction (Bellard et al. 2012). The WUE of plants was mainly driven by climate (Sheng et al. 2011). Therefore, the responses of WUE to climatic changes in three forestry regions of China were analyzed in this paper. In this paper, the WUE was negatively correlated with the temperature in the northeast and southeast forest regions. The temperature in the northeast forest region had an abrupt change in 1989. In fact, the temperature there increased from 1981 and increased significantly after 1990. The increase in temperature decreased the forest WUE in the northeast forest region during 1982–1999. In the southwest forest region, the WUE was positively correlated with the temperature. When the temperature increased by 1 °C, the increase rate of WUE slowed down sharply. In the southwest and southeast forest regions, the temperature increased remarkably from around 2001 and 2002. Therefore, in the southeast forest region, the regions presenting WUE decreasing trends increased from 2000 to 2019. Overall, the annual mean WUE after 2000 was higher than that before 2000, and the forest WUE increased in almost all regions of the study areas during 1961–2019. Some studies found that temperature increased while WUE of forest ecosystems decreased in the northeast region as well (Niu et al. 2011; Yu et al. 2008; Zhang et al. 2014). Yu et al. (2008) reported that air temperature increased while WUE of forest ecosystems decreased in Eastern China. Niu et al. (2011) revealed that climate warming could decrease the ecosystem WUE in Northern China. Zhang et al. (2014) found that the temperature changes negatively influenced WUE in the north and east of East Asia. However, some researchers got the opposite results. Zhang et al. (2016) simulated the temporal and spatial changes of WUE in the alpine area of Southwestern China and found that there were significant negative correlations between the WUE and temperature. Zhang et al. (2012) found that the correlation between WUE and temperature exhibited high negative in subtropical zones.

Table 5 The land use transition matrix in the southeast forest region (area, unit: km^2)

		2018						
		Cultivated land	Forests	Grasslands	Waters	Construction land	Unused land	Decrease
1980	Cultivated land	3841	113,580	613	176	280	6	114,655
	Forests	9617	639,950	3656	671	706	13	14,663
	Grasslands	614	46,774	960	39	41	2	47,470
	Waters	113	6326	20	94	13	0	6472
	Construction land	104	3,770	12	8	39	0	3894
	Unused land	8	188	0	0	0	1	196
	Increase	10,456	170,638	4301	894	1040	21	

The WUE displayed a negative relationship with precipitation in the study regions, especially to the decrease of precipitation. The sensitivity of WUE to precipitation reduction was highest in the artificial forest region and lowest in the northeast forest region. Many researchers got the same conclusion (Yu et al. 2008; Zhang et al. 2014). Yu et al. (2008) and Zhang et al. (2014) reported that precipitation increased while forest WUE decreased in the north and east of China. However, Zhang et al. (2016) found that there were significant positive correlations between WUE and precipitation in 34.1% of the alpine area in Southwest China during 1954–2010. Niu et al. (2011) also revealed that, in Northern China, the ecosystem WUE increased with increasing precipitation.

Human activities were stronger than those in the former 20 years (Chen et al. 2014). Chen et al. (2017b) revealed that human activities were the main driver affecting the NPP. Zou et al. (2017) discovered that the influence of human activities on ET was dramatically greater than that of climatic change. Therefore, human activities could influence forest WUE as well (Jiang et al. 2007). However, most studies focused on the response of NPP and ET to human activities, few studies on the responses of forest WUE to human activities directly. In this paper, WUE_{NDVI} was applied to explore the impacts of climatic changes and human activities on WUE. In the northeast, southwest, and southeast forest regions, the area of forests that converted into unused land was 1657 km^2, 581 km^2, and 13 km^2, respectively. Therefore, the forest fire on May 6, 1987, could have a certain influence on the northeast forest region. However, five key national ecological projects were established in three forestry regions of China. In the northeast forest region during 1982–1999, the NPP and WUE decreased while the NDVI and WUE_{NDVI} increased. From 1980 to 2018, the net increase of forest area in the northeast, southwest, and southeast forest regions was 78,766 km^2, 115,590 km^2, and 155,975 km^2. In general, the implementation of ecological projects could alleviate the degradation of forests. The greatest contributor was cultivated land (193,546 km^2). It indicated that the Returning Farmland to Forest project was being carried out steadily. The variations of WUE and WUE_{NDVI} were different in the northeast forest region, while basically the same in the southwest and southeast forest regions. Therefore, human activities had the greatest impact on WUE in the northeast forest region. However, in this paper, climatic changes were simply divided into temperature changes and precipitation variations. The detailed responses of WUE on human activities like ecological projects and other climatic changes, such as the varieties of atmospheric CO_2 and atmospheric nitrogen deposition, should be further studied.

5 Conclusions

In this paper, the responses of the forest WUE in three forestry regions of China to the climatic changes and human activities were analyzed from 1961 to 2019. The main findings of this study could be summarized as follows:

(1) The forest WUE and WUE_{NDVI} decreased from northwest to southeast over the whole three forestry regions of China. Overall, the spatial changes of WUE were very gentle in the artificial forest region, while fluctuated acutely in the two natural forest regions. The WUE of the southwest forest region increased with the increase of elevation, while the forest WUE in the southeast forest region increased with the decrease of elevation. In general, the annual mean WUE after 2000 was higher than that before 2000, and the forest WUE increased in almost all regions of the study areas during 1961–2019.

(2) The WUE was negatively correlated with the temperature in the northeast and southeast forest regions while it was positively correlated with the temperature in the southwest forest region. In the northeast forest region, the temperature rose since 1981 resulted in a decrease in the forest WUE during 1982–1999. When the temperature increased by 1 °C, the increase rate of WUE in the southwest forest region slowed down significantly. The WUE in the study regions displayed a negative relationship with precipitation, especially to the decreasing of precipitation. The sensitivity of WUE to the reduction of precipitation was highest in the artificial forest region and lowest in the northeast forest region.

(3) In the artificial forest region, the forest WUE and WUE_{NDVI} were the lowest but the net increase in forest area (155,975 km^2) was the largest. The WUE and WUE_{NDVI} in the northeast forest region were the highest, while the net increase of forest area (78,766 km^2) there was the lowest during 1980–2018. The variations of WUE and WUE_{NDVI} only presented different trends in the northeast forest region. Therefore, human activities had the greatest impact on WUE in the northeast forest region. In the northeast forest region during 1982–1999, the NPP and WUE decreased while the NDVI and WUE_{NDVI} increased. Human activities and climatic change were two main factors of the carbon cycle of terrestrial ecosystems, which have had complex and interactive effects on forest WUE. Therefore, the lumped influences of climate change and human activities on WUE should be further researched.

Acknowledgements This paper is financially supported by The National Key Research and Development Project of China (Grant NO. 2019YFC0409004) and National Natural Science Foundation of China (Grant NO. 91747203 and 41971025). The project is supported by the Priority Academic Program Development of Jiangsu Higher Education Institutions (PAPD). We would like to thank the National Climate Centre in Beijing for providing valuable climate datasets.

Author contribution J.T. wrote and revised the original draft. Z.Z., R.K., and F.Z. provided the datasets including the required supporting geoinformation software needed for the analyses; B.Z. and X.C. cooperated in designing and improving the concept of the research project and related processes; J.T. and S.J. conducted the data processing and analysis. All the authors participated actively in preparing and reviewing the manuscript.

Declarations

Conflicts of interest The authors declare no conflict of interest.

References

Asrar G, Fuchs M, Kanemasu ET, Hatfield JL (1984) Estimating absorbed photosynthetic radiation and leaf area index from spectral reflectance in wheat. *Agron J* 76:300–306

Babst F, Poulter B, Trouet V, Tan K, Neuwirth B, Wilson R, Carrer M, Grabner M, Tegel W, Levanic T, Panayotov M, Urbinati C, Bouriaud O, Ciais P, Frank D (2013) Site- and species-specific responses of forest growth to climate across the European continent. *Glob Ecol Biogeogr* 22(6):706–717

Bellard C, Bertelsmeier C, Leadley P, Thuiller W, Courchamp F (2012) Impacts of climate change on the future of biodiversity. *Ecol Lett* 15(4):365–377

Chang J, Tian J, Zhang Z, Chen X, Chen Y, Chen S, Duan Z (2018) Changes of grassland rain use efficiency and NDVI in Northwestern China from 1982 to 2013 and its response to climate change. *Water* 10(11):1689–1708

Chen B, Zhang X, Tao J, Wu J, Wang J, Shi P, Zhang Y, Yu C (2014) The impact of climate change and anthropogenic activities on alpine grassland over the Qinghai-Tibet Plateau. *Agric For Meteorol* 189-190:11–18

Chen T, Peng L, Liu S, Wang Q (2017a) Spatio-temporal pattern of net primary productivity in Hengduan Mountains area, China: impacts of climate change and human activities. *Chin Geogr Sci* 27(6):948–962

Chen X, Mo X, Hu S, Liu S (2017b) Contributions of climate change and human activities to ET and GPP trends over North China Plain from 2000 to 2014. *J Geogr Sci* 27(6):661–680

Fensholt R, Rasmussen K (2011) Analysis of trends in the Sahelian 'rain-use efficiency' using GIMMS NDVI, RFE and GPCP rainfall data. *Remote Sens Environ* 115(2):438–451

Gower ST, McMurtrie RE, Murty D (1996) Aboveground net primary production decline with stand age: potential causes. *Trends Ecol Evol* 11(9):378–382

Hanane S, Cherkaoui SI, Magri N, Yassin M (2018) Bird species richness in artificial plantations and natural forests in a North African agro-forestry system: assessment and implications. *Agrofor Syst*

Holm AM, Cridland SW, Roderick ML (2003) The use of time-integrated NOAA NDVI data and rainfall to assess landscape degradation in the arid shrubland of Western Australia. *Remote Sens Environ* 85(2):145–158

Hu Z, Wu G, Zhang L, Li S, Zhu X, Zheng H, Zhang L, Sun X, Yu G (2017) Modeling and partitioning of regional evapotranspiration using a satellite-driven water-carbon coupling model. *Remote Sens* 9(1):54–74

Lieth H, Whittaker RH (1975) Primary productivity of the biosphere. Spring Verlag, Berlin Heidelberg New York

Liu CY, Dong XF, Liu YY (2015) Changes of NPP and their relationship to climate factors based on the transformation of different scales in Gansu, China. *Catena* 125:190–199

Morecroft MD, Taylor ME, Oliver HR (1998) Air and soil microclimates of deciduous woodland compared to an open site. *Agric For Meteorol* 90(1):141–156

Niu SL, Xing XR, Zhang Z, Xia JY, Zhou XH, Song B, Li LH, Wan SQ (2011) Water-use efficiency in response to climate change: from leaf to ecosystem in a temperate steppe. *Glob Chang Biol* 17(2):1073–1082

Pan Y, Birdsey RA, Fang J, Houghton R, Kauppi PE, Kurz WA, Phillips OL, Shvidenko A, Lewis SL, Canadell JG, Ciais P, Jackson RB, Pacala SW, McGuire AD, Piao S, Rautiainen A, Sitch S, Hayes D (2011) A Large and persistent carbon sink in the world's forests. *Science* 333(6045):988–993

Pan Y, Zhang C, Gong H, Yeh PJF, Shen Y, Guo Y, Huang Z, Li X (2017) Detection of human-induced evapotranspiration using GRACE satellite observations in the Haihe River basin of China. *Geophys Res Lett* 44(1):190–199

Rafique R, Zhao F, de Jong R, Zeng N, Asrar GR (2016) Global and regional variability and change in terrestrial ecosystems net primary production and NDVI: a model-data comparison. *Remote Sens* 8(3): 177–192

Shao W, Cai J, Wu H, Liu J, Zhang H, Huang H (2017) An assessment of carbon storage in China's arboreal forests. *Forests* 8(4):110–123

Sheng WP, Ren SJ, Yu GR, Fang HJ, Jiang CM, Zhang M (2011) Patterns and driving factors of WUE and NUE in natural forest ecosystems along the North-South Transect of Eastern China. *J Geogr Sci* 21(4):651–665

Sun, F. B. (2007) Study on watershed evapotranspiration based on the Budyko hypothesis, 2007: 157.

Wang H, Li XB, Long HL, Gai YQ, Wei DD (2009) Monitoring the effects of land use and cover changes on net primary production: a case study in China's Yongding River basin. *For Ecol Manag* 258(12):2654–2665

Wright SJ (2005) Tropical forests in a changing environment. *Trends Ecol Evol* 20(10):553–560

Xiao FJ, Ouyang H, Zhang Q, Fu BJ, Zhang ZC (2004) Forest ecosystem health assessment and analysis in China. *J Geogr Sci* 14(1):18–24

Xiao JF, Sun G, Chen JQ, Chen H, Chen SP, Dong G, Gao SH, Guo HQ, Guo JX, Han SJ, Kato T, Li YL, Lin GH, Lu WZ, Ma MG, McNulty S, Shao CL, Wang XF, Xie X, Zhang XD, Zhang ZQ, Zhao B, Zhou GS, Zhou J (2013) Carbon fluxes, evapotranspiration, and water use efficiency of terrestrial ecosystems in China. *Agric For Meteorol* 182-183:76–90

Xu LK, Hsiao TC (2004) Predicted versus measured photosynthetic water-use efficiency of crop stands under dynamically changing field environments. *J Exp Bot* 55(407):2395–2411

Yu GR, Xia S, Wang QF, Liu YF, Guan DX, Yan JH, Sun XM, Zhang LM (2008) Water-use efficiency of forest ecosystems in eastern China and its relations to climatic variables. *New Phytol* 177(4): 927–937

Zhang FM, Ju WM, Shen SH, Wang SQ, Yu GR, Han SJ (2014) How recent climate change influences water use efficiency in East Asia. *Theor Appl Climatol* 116(1-2):359–370

Zhang Z, Jiang H, Liu JX, Zhou GM, Liu SR (2012) Assessment on water use efficiency under climate change and heterogeneous carbon dioxide in China terrestrial ecosystems. *Procedia Environ Sci* 13: 2031–2044

Zou M, Niu J, Kang S, Li X, Lu H (2017) The contribution of human agricultural activities to increasing evapotranspiration is significantly greater than climate change effect over Heihe agricultural region. *Sci Rep* 7(1):1–14

Jiang Y, Ma Y, Chen W, Wang P, Song F, Fang C, Wang G (2007) Review on influence factor and improvement way of crop water use efficiency. *Chin Agricult Sci Bull* 23(9):269–273

Sun YL, Yan XD, Xie DT, Wei CF (2007) Application of LPJ model in simulating vegetation distribution of China. *J Southwest Univ* 29(11):86–92

Zhang YD, Pang R, Gu FX, Liu SR (2016) Temporal-spatial variations of WUE and its response to climate change in alpine area of southwestern China. *Acta Ecol Sin* 36(6):1515–1525